High-rate capability of $Li_3V_2(PO_4)_3$/C composites prepared via a polyvinylpyrrolidone-assisted sol–gel method

Hao Wang[a], Yajuan Li[a,*], Chenghuan Huang[b], Yuedan Zhong[a], Suqin Liu[a]

[a] College of Chemistry and Chemical Engineering, Central South University, Changsha 410083, China
[b] Hunan Changyuan Lico Co., Ltd, Changsha 410205, China

ARTICLE INFO

ABSTRACT

Carbon-coated monoclinic $Li_3V_2(PO_4)_3$ (LVP/C) cathode materials are successfully prepared via a polyvinylpyrrolidone (PVP)-assisted sol–gel method. LVP/C composites are investigated by X-ray diffraction (XRD), X-ray photoelectron spectroscopy (XPS), scanning electron microscopy (SEM), high-resolution transmission electron microscopy (HR-TEM) and electrochemical methods. The results indicate that the sample synthesized with 9 wt% PVP is coated with a carbon layer in a thickness of about 12 nm, which presents excellent rate capability and good cyclic performance. In the potential range of 3.0–4.3 V, it shows a capacity of 127.2 and 115.1 mAh g^{-1} at 1 and 10 C, respectively. Even at discharge rate of 20 C, it still has 81.8 mAh g^{-1} with 10.7% capacity loss after 120 cycles. The lithium diffusion coefficient of the as-prepared material is in the order of 10^{-8} cm^2 s^{-1}. Our experiment results demonstrate that the LVP/C composites prepared via a PVP-assisted sol–gel method can be an attractive candidate as cathode materials in high-power lithium-ion batteries.

1. Introduction

Recently, lithium metal phosphates, which are considered as new generation of cathode materials for lithium-ion batteries, have attracted much research interest, such as orthorhombic $LiFePO_4$ and monoclinic $Li_3V_2(PO_4)_3$ [1,2]. Among them, monoclinic $Li_3V_2(PO_4)_3$ is a potential cathode material due to its high ionic diffusion coefficient, high operating voltage, high theoretical capacity (197 mAh g^{-1}) and high safety performance [3–6].

However, $Li_3V_2(PO_4)_3$ has an intrinsic low electronic conductivity (2.4 × 10^{-7} S cm^{-1} at room temperature), which largely limits its rate performance [7]. In order to overcome this restriction, various approaches have been used, including alien metal doping [8–10] and coating with electronically conductive agents, such as carbon [4,11–16] and Ag [17]. Carbon coating, which is usually realized by introducing an organic precursor in the starting materials, is regarded as an effective way to improve the conductivity of $Li_3V_2(PO_4)_3$. Further, the residual carbon from the pyrolysis of the organic precursor can also provide a network to limit the agglomeration of the $Li_3V_2(PO_4)_3$ particles and suppress particle growth during synthesis process. Further reducing particle size would improve the rate capability of the $Li_3V_2(PO_4)_3$ electrode due to the decrease of lithium ion diffusion and electron transportation distances [14].

The effectiveness of surface carbon depends on the carbon sources and synthetic routes [18,19]. Recently, Qiao et al. [20] synthesized $Li_3V_2(PO_4)_3$/C by a carbon-thermal reduction method using polyvinyl alcohol as a carbon source. Yuan et al. [21] reported a fast sol–gel method based on spontaneous chemical reactions to prepare $Li_3V_2(PO_4)_3$/C, which exhibited outstanding electrochemical performances. Polyvinylpyrrolidone (PVP), known as a non-ionic surfactant, is a perfect carbon coating source. When it is dissolved in water, the polarity of the water can be reduced, which results in homogeneous distribution of carbon [22]. In addition, PVP has excellent wetting properties and readily forms films in solution so that smooth and homogeneous carbon coating can be formed during sintering process. However, no studies have yet reported about the synthesis of LVP/C by a PVP-assisted sol–gel method.

In this work, we firstly introduced a PVP-assisted sol–gel method to synthesize LVP/C composites and investigated the structure and electrochemical performances (especially the high-rate capability) of the material. The lithium ion diffusion coefficient of as-prepared LVP/C composite was also investigated by cyclic voltammetry (CV) method.

2. Experimental

LVP/C composites were synthesized via a PVP-assisted sol–gel route, using V_2O_5, $NH_4H_2PO_4$, Li_2CO_3, oxalic acid and PVP as starting materials. All the starting materials were of analytical grade and used as received. Oxalic acid was used as a reducing agent, and PVP was used as a chelating reagent and carbon source. Firstly, V_2O_5

* Corresponding author. Tel.: +86 731 8887 9850; fax: +86 731 8887 9850.
E-mail address: yajuanli@csu.edu.cn (Y. Li).

and oxalic acid in a mol ratio of 1:3 were dissolved in deionized water under magnetic stirring at 70 °C until a clear green solution was formed, and then a mixture of stoichiometric amounts of $NH_4H_2PO_4$ and Li_2CO_3 were added to the solution. Subsequently, aqueous solution of appropriate amount of PVP (4, 9 and 13 wt%, labeled as the LVP/C4, LVP/C9 and LVP/C13, respectively) was added slowly to the above solution with stirring. The mixture was continuingly stirred at 70 °C to remove the excess water so that a gel was obtained. Then, the obtained gel was dried at 80 °C in an air oven and pre-heated at 350 °C for 4 h under Ar atmosphere. Finally, the pre-heated material was ground and sintered at 750 °C for 8 h under Ar flow to yield $Li_3V_2(PO_4)_3$/C composites. For comparison, the $Li_3V_2(PO_4)_3$ without PVP was prepared in the same way, labeled as the LVP.

X-ray diffraction (XRD) measurement was carried out on a RigaKu D/max2550VB$^+$ 18 kW using graphite-monochromatized Cu Kα radiation (40 kV, 250 mA). X-ray photoelectron spectroscopy (XPS) was performed with a K-Alpha 1063 type analyzer with monochromatic Al Kα radiation (Electrophysics, Britain) to evaluate the oxidation states of elements in $Li_3V_2(PO_4)_3$/C composites. The particle morphology was observed by a JSM-6360-LV scanning electron microscopy (SEM) and a JEM-2010 transmission electron microscope (TEM). The content of carbon was determined by C-S 800 infrared carbon-sulfur analyzer. Electronic conductivity measurements were carried out by four-point probe method using an RTS-9 Digital Instrument.

Electrochemical performance of the $Li_3V_2(PO_4)_3$/C composites were investigated using CR2016 coin-type cell with a metallic lithium foil served as the anode. The cathode membrane was fabricated by mixing the LVP/C composite, acetylene black and polytetrafluoroethene (PTFE) in the weight ratio of 80:10:10 to form homogeneous slurry. The slurry was then cast onto an aluminum foil, and the coated electrodes were dried at 120 °C for 12 h in vacuum. The cathode and lithium foil anode were separated by a polypropylene micro-porous film (Celgard 2300). The electrolyte was 1 M $LiPF_6$ in a mixture of EC-DMC-DEC (volume ratio of 1:1:1). The coin cells were assembled in an argon-filled glove box (Mbraun, Unilab, Germany). The charge–discharge measurements were conducted on Land battery test system (Wuhan, China) at room temperature between 3.0 and 4.3 V (vs. Li/Li$^+$). Cyclic voltammetry tests were carried out on three-electrode cell on CHI 660C (Shanghai, China) electrochemical workstation at room temperature in the potential range of 3.0–4.3 V (vs. Li/Li$^+$).

3. Results and discussion

3.1. Sample preparation and characterization

The XRD patterns of the $Li_3V_2(PO_4)_3$/C composites synthesized with different PVP contents are shown in Fig. 1. It can be clearly seen that all the XRD patterns of these samples are similar. All the diffraction lines can be assigned to a single phase of $Li_3V_2(PO_4)_3$ and indexed well as monoclinic structure with the space group of P2$_{1/n}$, which are consistent with the previous reports [4,5,23]. There is no evidence of diffraction peaks for carbon generated from PVP due to the amorphous state of the carbon or the low carbon content in these composites, which does not influence the crystalline structure of $Li_3V_2(PO_4)_3$.

Taking the XPS patterns of LVP/C9 as representation, the oxidation states of the elements in LVP/C are shown in Fig. 2a. All elements in $Li_3V_2(PO_4)_3$/C can be confirmed using XPS analysis, including O 1s, V 2p, C 1s, P 2s, P 2p and Li 1s. Fig. 2b shows the V 2p XPS core level. The V 2p XPS core level fits to a dominant single peak with a binding energy of 516.8 eV. Hence it can be concluded that the oxidation state of V in the $Li_3V_2(PO_4)3$/C composite is V^{3+} [8].
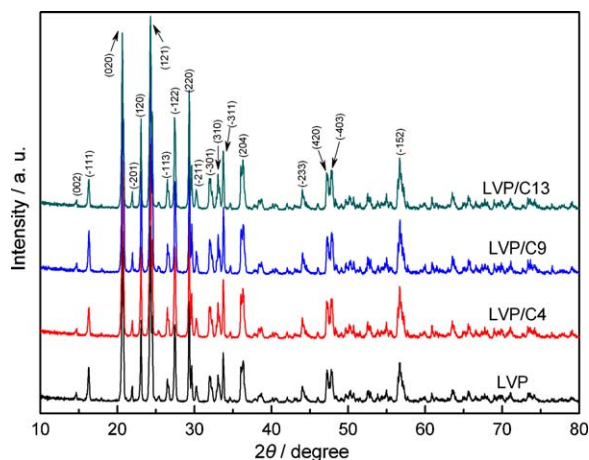

Fig. 1. XRD patterns of LVP, LVP/C4, LVP/C9 and LVP/C13.

In Fig. 2c, the C 1s spectrum at BE value of 284.6 eV is corresponded to sp^2 C—C bonds [24], indicating that PVP was decomposed into carbon during the calcinations. However, the lithium peak at a binding energy of 55.2 eV is much weaker. The possible reason is that the sensitivity of the equipment is not high enough to detect this lithium peak [25].

Fig. 3 shows the SEM images of the as-synthesized powders prepared with different PVP contents. In Fig. 3a, the particle size of the sample synthesized without PVP is obviously larger than those of samples synthesized with PVP (Fig. 3b–d), which indicates that the presence of PVP in the precursor has a notable effect on the morphology and particle size of the materials during sintering. Apart from fine particles, some relatively large clusters are existed in Fig. 3a. When the PVP content increases to 4 wt% (Fig. 3b), the particle size is smaller with some small clusters, which means that the distribution of the carbon is still not homogeneous. It can be clearly seen in Fig. 3c that an increase in the amount of 9 wt% PVP results in much smaller particle size with relatively minimal agglomeration. In particles with smaller, uniform and well-dispersed particle size, it is believed to be advantaged to the electrochemical performance of $Li_3V_2(PO_4)_3$/C composites for it can provide short diffusion paths and fast diffusion rates along their grain boundaries. In Fig. 3d, though there is a further decrease in the particle size, the agglomeration is serious in the case of 13 wt% PVP.

In order to check the carbon configuration on the surface of the $Li_3V_2(PO_4)_3$ particles and understand fully about the microstructure of the composite, TEM analysis of the $Li_3V_2(PO_4)_3$/C particles was conducted. It can be seen that the LVP/C9 particle, which has several hundred nanometers in size, is coated with a uniform amorphous carbon layer in a thickness of about 12 nm (Fig. 4c and d). The network formation of carbon appears in the interstitial grain-boundary region, which can inhibit the growth of the $Li_3V_2(PO_4)_3$ grain and provide good contact between the particles. In Fig. 4a and b the thickness of the carbon coating on the LVP/C4 and LVP/C13 particles is about 7 and 20 nm, respectively. Furthermore, it can be clearly seen in Fig. 4b that multilayer carbon coating with irregular shape tightly wraps around the LVP particles. According to the elemental analysis, the carbon content of LVP/C4, LVP/C9, LVP/C13 is 0.98, 2.05 and 3.48 wt%, respectively. The above microstructure of amorphous carbon coating layer is believed to have a major influence on the rate capacity [26,27].

3.2. Electrochemical performance

To further understand the effect of PVP addition on the electrochemical performance of the $Li_3V_2(PO_4)_3$/C composite, the rate
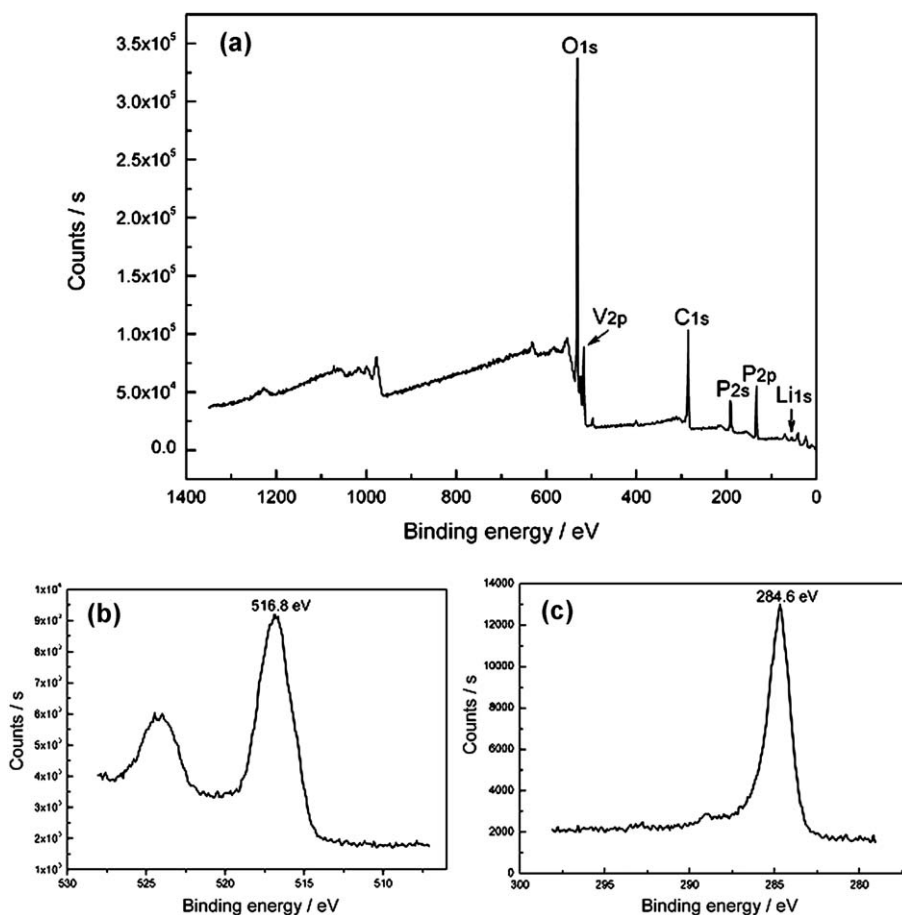
Fig. 2. XPS spectra of LVP/C9 (a), XPS core level of V 2p (b) and C 1s (c).

capability in the potential range of 3.0–4.3 V is shown in Fig. 5. It can be obviously seen that the rate capability of the PVP added $Li_3V_2(PO_4)_3$/C composites is much better than that of the $Li_3V_2(PO_4)_3$ synthesized without PVP. The LVP/C9 exhibits the best rate capability. Its discharge capacity slightly decreases from 131.4 mAh g^{-1} at 0.2 C to 118.1 mAh g^{-1} at 5 C. After 30 cycles, the capacity retention of the LVP/C9 is 98.9% (116.8 mAh g^{-1}) at 5 C, indicating its good cycling performance. Furthermore, a capacity
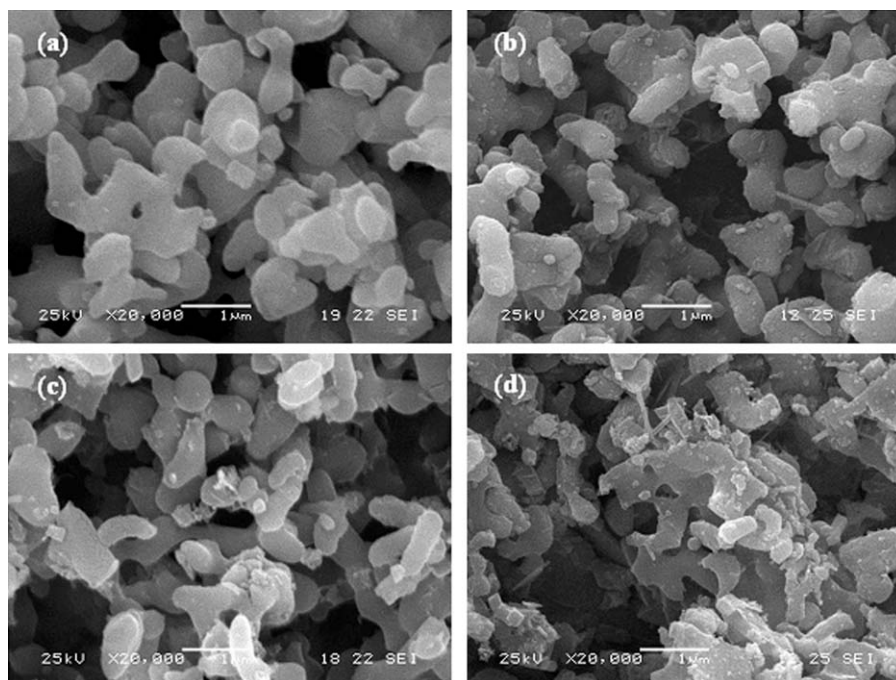

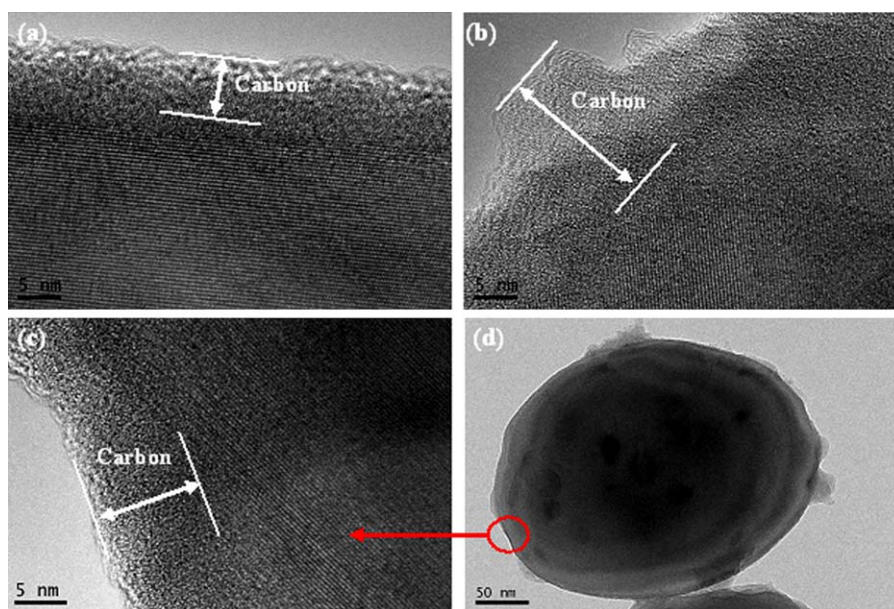**Fig. 3.** SEM images of LVP (a), LVP/C4 (b), LVP/C9 (c) and LVP/C13 (d).

Fig. 4. HRTEM images of LVP/C4 (a), LVP/C13 (b) and LVP/C9 (c and d).

of 128.6 mAh g^{-1} can be still obtained when the rate returns to 0.2 C again after 100 cycles, exhibiting the excellent reversibility of the composite. In contrast, the LVP/C4 and LVP/C13 have lower discharge capacity at 5 C, which is 80.1 and 94.4 mAh g^{-1}, respectively. The reasons may be as follows. For LVP/C4, the lower content of PVP in its synthesis is not enough for getting the material with fine particles. The large particle size may be the major reason for its lower capacity rate. For LVP/C13, the active material content is relatively decreased with the increase of carbon content, which results in the lower capacity. As its rate capability is concerned, the particle size and the thickness of carbon coating layer are the significant factors determining the kinetics. The LVP/C9 has fine particle size and optimal carbon coating thickness, which result in its better rate capability. Whereas, the relatively large particle size of LVP/C4 (seen in Fig. 3b) and too thick carbon-coating layer of LVP/C13 (seen in Fig. 4b) are both impeding factors for the diffusion of lithium ion, which cause a relatively large resistance [28,29].

To further affirm the electrochemical kinetics of LVP/C, the high rate charge–discharge and cyclic voltammetry tests were conducted. Fig. 6 shows the charge–discharge curves and cyclic performance of LVP/C9 at different rates in the potential range

of 3.0–4.3 V. It can be clearly seen in Fig. 6a that at 1 C the curve exhibits three charge flat plateaus and correspondingly three discharge ones, which are identified as the two-phase transition processes during the electrochemical reactions [3–6]. The Li$_3$V$_2$(PO$_4$)$_3$/C composite exhibits excellent rate capability with
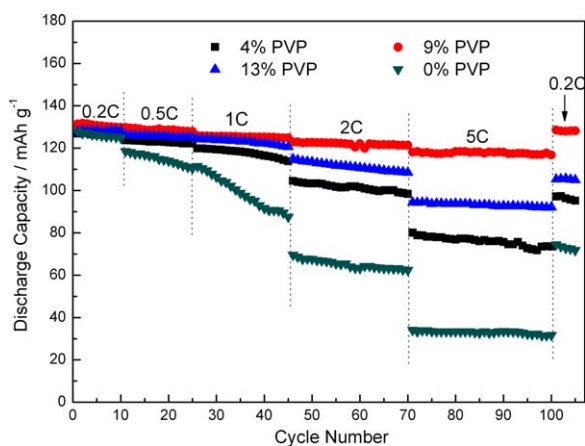

Fig. 5. The rate capacity of Li$_3$V$_2$(PO$_4$)$_3$/C composites synthesized with 0–13 wt% PVP in the potential range of 3.0–4.3 V.
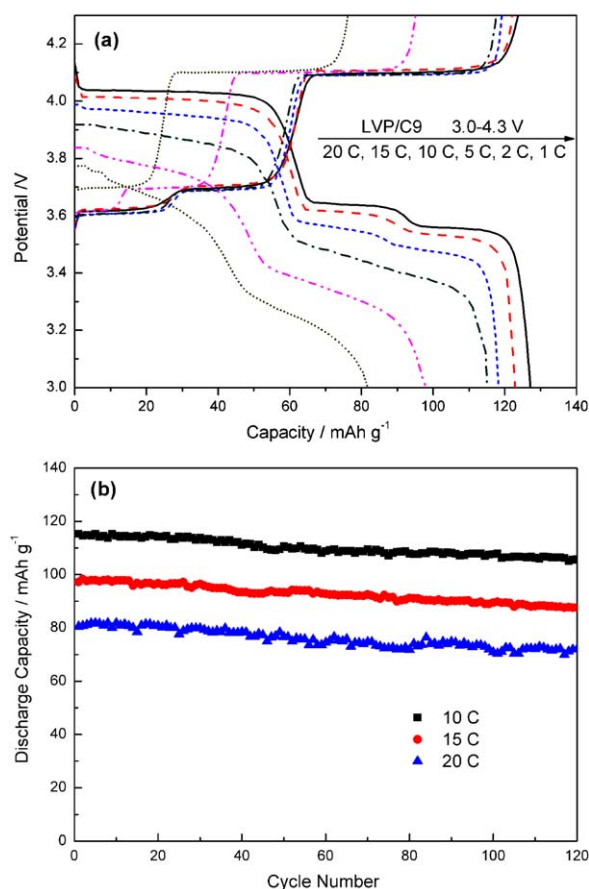
Fig. 6. The charge–discharge curves and cyclic performance of the LVP/C9 in the potential range of 3.0–4.3 V.
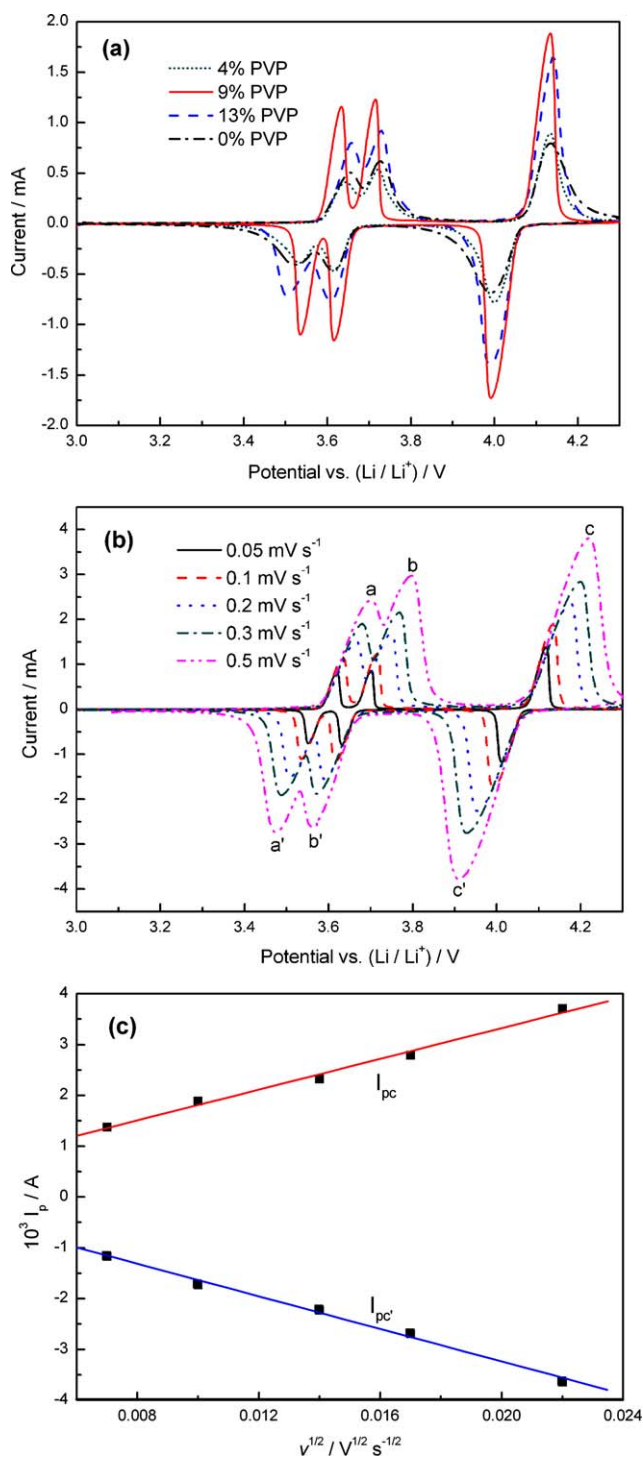
Fig. 7. CV curves of $Li_3V_2(PO_4)_3$/C composites synthesized with 0–13 wt% PVP at 0.1 mV s^{-1} in the potential range of 3.0–4.3 V (a), CV curves of LVP/C9 at various scanning rates (b) and peak current I_p as a function of square root of scan rate $\upsilon^{1/2}$ (c).

the discharge capacities of 127.2, 122.9, 118.3, 115.1, 98.6 and 81.8 mAh g^{-1} at the rate of 1, 2, 5, 10, 15 and 20 C, respectively. A good cycling capability of LVP/C9 can be seen in Fig. 6b with 8.2%, 9.9% and 10.7% capacity loss after 120 cycles at the rate of 10, 15 and 20 C, respectively. The high-rate capacity and excellent cycling capability could be attributed to the enhanced electronic conductivity of the material as a result of the carbon coating layer in situ formed on the surface of the particles (seen in Fig. 4c and d). Further, the carbon coating can decrease the

charge-transfer impedance [30]. Electronic conductivity measurement illustrates that the electronic conductivity of the LVP/C9 is 2.58×10^{-2} S cm^{-1} at 300 K, which is much higher than that of pure $Li_3V_2(PO_4)_3$.

Cyclic voltammogram test is an effective method to research the kinetics. The initial CV curves of the $Li_3V_2(PO_4)_3$/C composites between 3.0 and 4.3 V at a scan rate of 0.1 mV s^{-1} are shown in Fig. 7a. All the electrodes present three couples of oxidation and reduction peaks in the potential range of 3.0–4.3 V. It can be seen from Fig. 7a that the curves have the same shape, which indicates the similar redox behavior in the electrodes. As for cyclic voltammogram, the potential interval between anodic peak and cathodic one is an important parameter to evaluate the electrochemical reaction reversibility. In Fig. 7a, the CV curve of LVP/C9 electrode has the narrowest separation between the anodic peak and the cathodic one. It suggested that the LVP/C9 electrode showed the best electrochemical reversibility and the electrode reaction was improved by carbon coating, indicating its excellent kinetics. The carbon coating layer is not necessarily related to the best electrochemical reversibility, but the too thick of carbon layer may result in the polarization of electrode. But it still should be pointed out that the electrochemical performances of $Li_3V_2(PO_4)_3$/C composites are better than that of LVP. The CV measurement is also widely used to investigate the apparent diffusion coefficient of lithium ion [12,31]. Fig. 7b shows the CV curves of the LVP/C9 at various scan rates in 3.0–4.3 V. With the scan rate increases, the peak current increases, meanwhile the cathodic and anodic peaks move to lower and higher potentials, respectively, which indicates the irreversibility of the electrochemical reactions due to the electrode polarization at larger scan rates. Herein, the classical Randles-Sevchik equation for a semi-infinite diffusion of Li$^+$ into $Li_3V_2(PO_4)_3$ can be applied. The formula can be written as [32]:

$$I_p = 2.69 \times 10^5 n^{3/2} A D^{1/2} C_0 \upsilon^{1/2} \tag{1}$$

where I_p is the peak current (A), n is the charge-transfer number, A is the active surface area of the electrode (0.64 cm^2), D is the diffusion coefficient of the Li$^+$ ion (cm^2 s^{-1}), C_0 is the concentration of Li$^+$, υ is the scan rate (V s^{-1}). The CV curves are composed of three redox couples which are labeled as a/a′, b/b′ and c/c′, respectively. In this work, we select the peaks c and c′, which are single peak in the CV curve, to calculate the D values according to formula (1). As shown in Fig. 7c, I_p is indeed proportional to $\upsilon^{1/2}$ confirming a diffusion-controlled behavior. From the slope of I_p vs. $\upsilon^{1/2}$, the apparent diffusion coefficients D_c (c peak) and $D_{c'}$ (c′ peak) could be calculated to be 5.74×10^{-8} and 6.43×10^{-8} cm^2 s^{-1}, respectively. The D values at these redox peaks are very close, indicating excellent reversibility of the material.

4. Conclusions

The carbon-coated $Li_3V_2(PO_4)_3$ cathode material has been successfully synthesized by a PVP-assisted sol–gel method. The suitable carbon nano-layer on $Li_3V_2(PO_4)_3$ particles suppressed the particle growth and enhanced the electronic conductivity of the material, resulting in its excellent high-rate performance. The sample synthesized with 9 wt% PVP exhibits excellent rate capability. At the rate of 10 and 20 C the discharge capacity of the material is 115.1 and 81.8 mAh g^{-1}, respectively. This sample also exhibits excellent kinetics. The lithium diffusion coefficient is in the order of 10^{-8} cm^2 s^{-1}. All these results illustrate that such a PVP-assisted sol–gel processed $Li_3V_2(PO_4)_3$/C composite can be a promising cathode material for high-powder density lithium-ion batteries.

Acknowledgment

References

[1] S.Y. Chung, J.T. Bloking, Y.M. Chiang, Nat. Mater. 1 (2002) 123–128.
[2] S.F. Yang, P.Y. Zavalij, M.S. Whittingham, Electrochem. Commun. 3 (2001) 505–508.
[3] M.Y. Saidi, J. Barker, H. Huang, J.L. Swoyer, G. Adamson, J. Power Sources 119 (2003) 266–272.
[4] H. Huang, S.-C. Yin, T. Kerr, N. Taylor, L.F. Nazar, Adv. Mater. 14 (2002) 1525–1528.
[5] S.-C. Yin, H. Grondey, P. Strobel, M. Anne, L.F. Nazar, J. Am. Chem. Soc. 125 (2003) 10402–10411.
[6] S.-C. Yin, H. Grondey, P. Strobel, H. Huang, L.F. Nazar, J. Am. Chem. Soc. 125 (2003) 326–327.
[7] Y.Q. Qiao, X.L. Wang, J.Y. Xiang, D. Zhang, W.L. Liu, J.P. Tu, Electrochim. Acta 56 (2011) 2269–2275.
[8] M.M. Ren, Z. Zhou, Y.Z. Li, X.P. Gao, J. Yan, J. Power Sources 162 (2006) 1357–1362.
[9] S.Q. Liu, S.C. Li, K.L. Huang, B.L. Gong, G. Zhang, J. Alloys Compd. 450 (2008) 499–504.
[10] Y.H. Chen, Y.M. Zhao, X.N. An, J.M. Liu, Y.Z. Dong, L. Chen, Electrochim. Acta 54 (2009) 5844–5850.
[11] Q.Q. Chen, J.M. Wang, Z. Tang, W.C. He, H.B. Shao, J.Q. Zhang, Electrochim. Acta 52 (2007) 5251–5257.
[12] T. Jiang, W.C. Pan, J. Wang, X.F. Bie, F. Du, Y.J. Wei, C.Z. Wang, G. Chen, Electrochim. Acta 55 (2010) 3864–3869.
[13] P. Fu, Y.M. Zhao, Y.Z. Dong, X.N. An, G.P. Shen, J. Power Sources 162 (2006) 651–657.
[14] A.Q. Pan, J. Liu, J.G. Zhang, W. Xu, G.Z. Cao, Z.M. Nie, B.W. Arey, S.Q. Liang, Electrochem. Commun. 12 (2010) 1674–1677.
[15] M.M. Ren, Z. Zhou, X.P. Gao, W.X. Peng, J.P. Wei, J. Phys. Chem. C 112 (2008) 5689–5693.
[16] Y.Q. Qiao, X.L. Wang, Y. Zhou, J.Y. Xiang, D. Zhang, S.J. Shi, J.P. Tu, Electrochim. Acta 56 (2010) 510–516.
[17] L. Zhang, X.L. Wang, J.Y. Xiang, Y. Zhou, S.J. Shi, J.P. Tu, J. Power Sources 195 (2010) 5057–5061.
[18] Y.Q. Qiao, X.L. Wang, Y.J. Mai, J.Y. Xiang, D. Zhang, C.D. Gu, J.P. Tu, J. Power Sources 196 (2011) 8706–8709.
[19] K. Nagamine, T. Honma, T. Komatsu, J. Power Sources 196 (2011) 9618–9624.
[20] Y.Q. Qiao, J.P. Tu, X.L. Wang, C.D. Gu, J. Power Sources 199 (2012) 287–292.
[21] W. Yuan, J. Yan, Z.Y. Tang, O. Sha, J.M. Wang, W.F. Mao, L. Ma, J. Power Sources 201 (2012) 301–306.
[22] S.W. Oh, S.T. Myung, S.M. Oh, C.S. Yoon, K. Amine, Y.K. Sun, Electrochim. Acta 55 (2010) 1193–1199.
[23] M.Y. Saidi, J. Barker, H. Huang, J.L. Swoyer, G. Adamson, Electrochem, Solid State Lett. 5 (2002) A149–A151.
[24] N.N. Sinha, N. Munichandraiah, ACS Appl. Mater. Int. 1 (2009) 1241–1249.
[25] Z.Y. Chen, C.S. Dai, G. Wu, M. Nelson, X.G. Hu, R.X. Zhang, J.S. Liu, J.C. Xia, Electrochim. Acta 55 (2010) 8595–8599.
[26] A.P. Tang, X.Y. Wang, S.Y. Yang, Mater. Lett. 62 (2008) 3676–3678.
[27] C.X. Chang, J.F. Xiang, X.X. Shi, X.Y. Han, L.J. Yuan, J.T. Sun, Electrochim. Acta 53 (2008) 2232–2237.
[28] R. Dominko, M. Bele, M. Gaberscek, M. Remskar, D. Hanzel, S. Pejovnik, J. Jamnik, J. Electrochem. Soc. 152 (2005) A607–A610.
[29] M. Gaberscek, R. Dominko, M. Bele, M. Remskar, D. Hanzel, J. Jamnik, Solid State Ionics 176 (2005) 1801–1805.
[30] Y.Z. Li, Z. Zhou, X.P. Gao, J. Yan, Electrochim. Acta 52 (2007) 4922–4926.
[31] L. Wang, X.Q. Jiang, X. Li, X.Q. Pi, Y. Ren, F. Wu, Electrochim. Acta 55 (2010) 5057–5062.
[32] A.J. Bard, L.R. Faulkner, Electrochemical Methods: Fundamentals and Applications, Wiley, New York, 1980, pp. 213–222.